HIGH-ENERGY ELECTRON SCATTERING ON ^{6}Li AND ^{12}C AS AN INCOHERENT SUPERPOSITION OF SINGLE-NUCLEON PROCESSES

U. GLAWE and U. STROHBUSCH
I. Institut für Experimentalphysik der Universität Hamburg, Germany

and

J. FRANZ, P. GROSSE-WIESMANN [1], G. GUZIELSKI, G. HUBER, G. MECKLENBRAUCK, W. MECKLENBRAUCK and E. RÖSSLE
Fakultät für Physik der Universität Freiburg, Breisgau, Germany

Received 30 August 1979

High-energy electro-excitation cross sections on ^{6}Li and ^{12}C in the region of the first nucleon resonance are compared with calculations in the impulse approximation. It is shown that the ^{6}Li and ^{12}C cross sections can be reproduced by an incoherent superposition of nucleon structure functions for $0.2 < Q^2 < 0.4$ GeV^2 and primary energies in the GeV range.

The influence of nuclear matter on the nucleon resonances has been discussed in several papers [1]. An unexpected experimental result is reported in refs. [2] and [3], where the cross section per nucleon for the Δ_{33} electro-excitation in the nuclei ^{6}Li and ^{12}C was observed to be significantly smaller than for free nucleons. This appears to be surprising, since the electron is expected to interact with single nucleons only, due to the short wave length of the transferred virtual photon in the kinematic region $0.2 < Q^2 < 0.4$ GeV^2 covered by these experiments.

This paper presents a reanalysis of the data of ref. [2] using a method developed in the course of our study of deep inelastic electron–nucleus scattering (invariant mass $W > 2$ GeV) [4] requiring knowledge of the cross sections in the resonance region. The method used is that of Atwood and West [5], but generalized to heavier nuclei.

The basic assumptions are:

(i) The one-photon exchange approximation holds also for electron scattering on complex nuclei.

(ii) The electron interacts with only one nucleon in the nucleus. The other nucleons remain unaffected. (impulse approximation).

(iii) The momentum distributions of the bound nucleons are described by the nuclear shell model.

(iv) The structure functions for free and bound nucleons are identical.

These assumptions are the same as those used in ref. [2]. Our analusis, however, differs from their method particularly in handling the Fermi motion. Instead of folding the nucleon cross sections with the Fermi motion, our procedure takes into account that only the hadron vertex is influenced by the Fermi motion, whereas the lepton vertex remains unaffected. The other main difference in the analysis lies in the description of the elementary processes. We describe the nuclear cross sections in a phenomenological manner, where we have fixed the parameters as far as possible. The authors of ref. [2] used a somewhat artificial partitioning of the cross sections with several parameters adjusted in the final fitting procedure.

In the one-photon exchange approximation the twofold differential cross section for electron–nucleon scattering is usually written as:

[1] Present address: MPI für Physik und Astrophysik, Munich, Germany.

$$\sigma = \mathrm{d}^2\sigma/\mathrm{d}E\mathrm{d}\Omega = \sigma_{\mathrm{Mott}}[W_2(Q_2, \nu) + 2W_1(Q^2, \nu)\tan^2(\theta_e/2)] \,. \quad (1)$$

Here θ_e is the electron scattering angle, W_1 and W_2 are the structure functions of the nucleon, Q_2 is the four-momentum transfer ($Q^2 > 0$) and ν is the energy transfer to the hadronic system.

Since the one-photon exchange approximation has also been proved valid for complex nuclei [6], the cross section for inclusive electron–nucleus scattering can be correspondingly factorized:

$$\sigma_A = \mathrm{d}^2\sigma_A/\mathrm{d}E\mathrm{d}\Omega = \sigma_{\mathrm{Mott}}[W_2^A(Q^2, \nu) + 2W_1^A(Q^2, \nu)\tan^2(\theta_e/2)] \,. \quad (2)$$

The structure functions W_1^A and W_2^A of the nucleus with mass number A are obtained by folding the nucleon structure functions with the momentum distribution of the interacting nucleon while Q^2 is fixed. It turns out that the structure function W_1^A of the nucleus is a function of both W_1 and W_2 of the free nucleons, whereas W_2^A depends only on W_2. The functional dependence reflects the kinematics of the scattering process including the Fermi motion and binding energy of the scattering nucleon. The contributions of the different shells to the nuclear structure functions W_1^A and W_2^A are calculated separately and summed according to the occupation number of the different shells. The complete deduction of W_1^A and W_2^A is given in basic form for the deuteron case in ref. [5] and in detail for complex nuclei in ref. [7].

For the calculations we took an empirical parametrization of the nucleon structure functions, whereby it is convenient to separate the nuclear cross section into two parts, namely the quasi-elastic and the inelastic contribution.

For the quasi-elastic part of the nuclear structure functions we used nucleon structure functions taken from the Rosenbluth formula with the electric and magnetic form factors of the nucleons given by the scaling law and the dipole fit.

An equivalent parametrization of inelastic electron–nucleon scattering does not exist. Therefore we used W_1 and W_2 extracted from measured inelastic cross sections of protons and deuterons [8]. In order to cover the region below $Q^2 = 0.15$ GeV^2, photoproduction data were included [9]. The structure functions for protons and neutrons were obtained in the kinematic region $Q^2 < 1.5$ GeV^2 and for invariant masses $W < 1.8$ GeV by interpolating the experimental data along lines of constant W. The quality of the interpolations was checked by reproducing independent measurements within the kinematic region defined above [7].

The procedure outlined here was applied to obtain the quasi-elastic and the inelastic parts of W_1^A and W_2^A for the nuclei ^{6}Li and ^{12}C within the kinematic region $Q^2 \leqslant 1.5$ GeV^2 and $\nu \leqslant 1.7$ GeV. Using the values of W_1^A and W_2^A, the cross sections for quasi-elastic and for inelastic scattering, σ_A^{quel} and σ_A^{inel}, respectively, were computed separately according to eq. (2).

For the comparison with the measured cross section, radiative processes have to be considered. Since the nuclear cross sections have been calculated for the whole kinematic region, the contributions of the radiative processes to the experimental cross section can be directly calculated. This was done by applying the formulas of Mo and Tsai [10]. The radiative tail of elastic electron–nucleus scattering has been estimated to be negligible for $Q^2 > 0.2$ GeV^2. In order to account for the experimental resolution FWHM = 0.025 GeV, the calculated cross sections were smeared by a gaussian distribution. A detailed description of the measurements is given in refs. [11] and [12].

The experimental cross section of the nucleus is parametrized as the sum of the two calculated contributions σ_A^{quel} and σ_A^{inel},

$$\sigma_A^{\mathrm{exp}} = C\left|\frac{A_{\mathrm{eff}}^{\mathrm{quel}}}{A}\,\sigma_A^{\mathrm{quel}} + \frac{A_{\mathrm{eff}}^{\mathrm{inel}}}{A}\,\sigma_A^{\mathrm{inel}}\right| \,.$$

For quasi-elastic scattering the impulse approximation is well established [5,13]. Since no Pauli blocking is expected [14] for $Q^2 > 0.2$ GeV^2 the effective number of nucleons for quasi-elastic scattering, $A_{\mathrm{eff}}^{\mathrm{quel}}$, is set equal to A. The only parameters left are C and $A_{\mathrm{eff}}^{\mathrm{inel}}/A$. The factor C accounts for systematic errors [15] in the absolute experimental cross sections and $A_{\mathrm{eff}}^{\mathrm{inel}}/A$ is a measure of the validity of the underlying model to be tested against the experiment. It should be unity if inelastic electron–nucleus scattering, as in the case of quasi-elastic scattering, can be described as an incoherent superposition of single-nucleon processes.

Fig. 1 compares our results with the experimental data of refs. [11] and [12]. The calculations reproduce

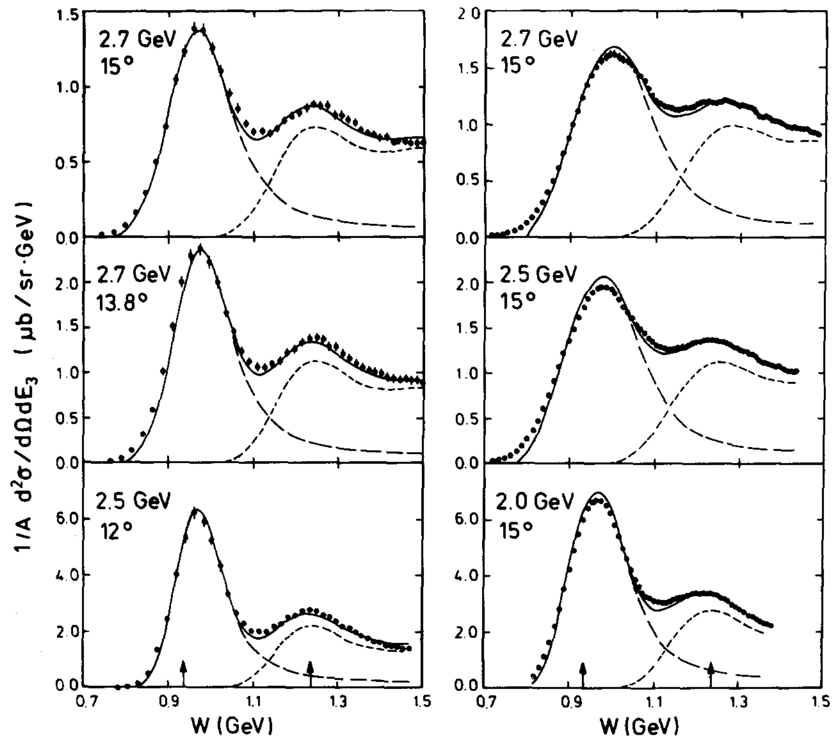

a. ^{6}Li b. ^{12}C

Fig. 1. Electron scattering cross section versus the invariant mass W for ^{6}Li and ^{12}C target nuclei. The long- and short-dashed lines represent the calculations for quasi-elastic and inelastic scattering, respectively. The solid line is the sum of both. The arrows indicate the masses of the proton and the Δ_{33} resonance.

the width and the shift of the peaks originating from the Fermi motion and binding energies of the nucleons [16]. For ^{6}Li the general agreement is good and no significant deviations from the experimental spectra are observed. The ^{12}C data differ from the calculations in the region of low invariant mass, and the minimum between quasi-elastic and inelastic scattering is more pronounced in the calculations. This is caused by the fact that the experimental spectra of ^{12}C are smoothed with gaussian distributions [12].

The values of $A_{\mathrm{eff}}^{\mathrm{inel}}/A$ obtained from the fit are listed in table 1 and are plotted versus $Q^2_{\Delta_{33}}$ in fig. 2. The mean values of $A_{\mathrm{eff}}^{\mathrm{inel}}/A$ are 0.97 and 1.01 for ^{6}Li and ^{12}C, respectively. With an estimated uncertainty of at least 10% for the extracted values (due to the uncertainties in the input data, particularly the neutron cross sections), we find no significant deviation of the effective mass number $A_{\mathrm{eff}}^{\mathrm{inel}}$ from the number of nucleons A composing the nuclei.

In summary, for ^{6}Li and ^{12}C in the kinematic region $W < 1.5$ GeV and $0.2 < Q^2 < 0.4$ GeV^2 for primary energies in the GeV range, the experimental cross sections are described in the impulse approximation by folding the nucleon structure function

Table 1
Values for $A_{\mathrm{eff}}^{\mathrm{inel}}/A$.

Target nucleus	E_1 (GeV)	θ_e	$Q_{\Delta_{33}}$ (GeV^2)	$A_{\mathrm{eff}}^{\mathrm{inel}}/A$ a)
^{6}Li	2.50	12.0	0.022	0.97
^{6}Li	2.70	13.8	0.348	0.97
^{6}Li	2.70	15.0	0.395	0.96
^{12}C	2.0	15.0	0.210	1.01
^{12}C	2.50	15.0	0.337	1.02
^{12}C	2.70	15.0	0.395	1.01

a) Errors estimated at 10%.

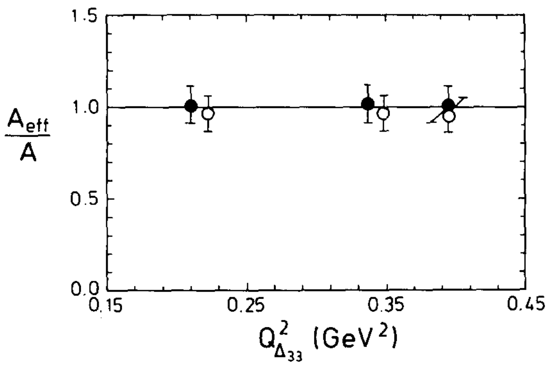

Fig. 2. A_{eff}^{inel}/A for ^{6}Li (○) and ^{12}C (•) versus Q^2 (GeV^2) at W = 1.236 GeV.

with the momentum distributions of the bound nucleons. Contrary to the results of ref. [2] the present analysis of the same data reveals no suppression of electro-excitation in the Δ_{33} region.

We wish to thank DESY for the hospitality and in particular the DESY-Rechenzentrum for their assistance during the numerical computations. This work has been supported by the Bundesministerium für Forschung und Technologie.

References

[1] M. Dillig and M.G. Huber, in: Mesonic effects in nuclear structure, eds. K. Bleuler et al. (B.I. Wissenschaftsverlag, 1975);
H. Arenhoevel and H.J. Weber, Springer Tracts in Modern Physics, Vol. 65 (1972);
A.M. Green, Rep. Prog. Phys. 39 (1976) 1109.
[2] F.H. Heimlich et al., Nucl. Phys. A231 (1974) 509.
[3] Yu.I. Titov and E.V. Stepula, Sov. J. Nucl. Phys. 15 (1972) 361.
[4] G. Huber, I. Blomqvist, P. David, J. Franz, B. Johnsson, G.G. Jonsson, H. Mommsen, R. Petersson, E. Rössle and U. Strohbusch, DESY Proposal 141 (1976).
[5] W.B. Atwood and G.B. West, Phys. Rev. D7 (1973) 773.
[6] S. Hartwig et al., Phys. Lett. 82B (1979) 297.
[7] P. Grosse-Wiesmann, Diplomarbeit, Freiburg (1978);
U. Glawe, Thesis, Hamburg (1979).
[8] M. Koebberling, J. Moritz, K.H. Schmidt, D. Wegener, D. Zeller, J. Bleckwenn and F.H. Heimlich, Kernforschungszentrum Karlsruhe, KFK Report 1822 (1973); Nucl. Phys. B82 (1974) 201.
[9] T.A. Armstrong et al., Phys. Rev. D5 (1972) 1640; Nucl. Phys. B41 (1972) 445.
[10] L.W. Mo and Y.S. Tsai, Rev. Mod. Phys. 41 (1969) 205.
[11] F.H. Heimlich, Thesis Freiburg (1973); DESY Internal Report F23/73/2 (1973).
[12] D. Zeller, Thesis Karlsruhe (1973); DESY Internal Report F23-73/2 (1973).
[13] K.C. Stanfield, C.R. Canizares, W.L. Faissler and F.M. Pipkin, Phys. Rev. C3 (1971) 1448.
[14] J. Bernabeu, Nucl. Phys. B49 (1972) 186.
[15] D. Zeller, private communication (1978).
[16] L.R.B. Elton and A. Swift, Nucl. Phys. A94 (1967) 52;
G. Tibell, D. Sundberg and P.U. Renberg, Ark. Fys. 25 (1963) 433.